Two-Dimensional Transition Metal Carbides and Nitrides (MXenes): Synthesis to Applications

Muhammad Zahir Iqbal and Saman Siddique

Abstract Recently, a novel family of two-dimensional materials, called MXenes, comprising of early transition metal nitrides and carbides was discovered with intriguing characteristics and potential applications. MXenes are synthesized by adopting various top down and bottom up approaches such as selective etching of "A" element from MAX phases result in a new MXene element, for instance, Ti_3C_2, V_2C, Ti_3CN, MoC_2, Ta_4C_3 etc. MXenes exhibit high metallic conductivity in which solid layers are bonded together with strong ionic, covalent and metallic bonds. The hydrophilic nature of MXene enhance its practical applications such as electrocatalyst, energy storage devices and in biomedical applications. Here, the chapter reviews the basic structure of newly discovered MXene materials, different synthesis techniques, structural, electrical and optical properties. Some potential applications in the field of biomedical, energy conversion and electrochemical energy storage systems and electrocatalyst are also presented in this chapter.

Keywords MXenes · Synthesis · Properties · Applications · Biomedical · Energy storage

1 Introduction

Two-dimensional materials (2DMs) have achieved a significant importance over the last decade due to exceptional structural, electrical and optical properties. Graphene was the first 2DM discovered in 2004 by Novoselov, comprising of atomically thin carbon sheets bonded covalently in a honeycomb structure [1]. Additionally, various two-dimensional materials have been synthesized such as hexagonal boron nitride (hBN) [2], silicene [3], arsenene [4], germanene, bismuthene [5, 6] and transition

M. Z. Iqbal (✉) · S. Siddique
Nanotechnology Research Laboratory, Faculty of Engineering Sciences, GIK Institute of Engineering Sciences and Technology, Topi, Khyber Pakhtunkhwa 23640, Pakistan
e-mail: zahir.upc@gmail.com

N. M. Mubarak et al. (eds.), *Contemporary Nanomaterials in Material Engineering Applications*, Engineering Materials,
https://doi.org/10.1007/978-3-030-62761-4_7

metal dichalcogenides [7]. Among various two-dimensional materials some are insulators such as hBN while some are semiconductors as transition metal dichalcogenides, silicene, arsenene and bismuthene. Two-dimensional materials are utilized in various scientific applications ranging from electronics to electrochemical energy storage and conversion devices such as field effect transistors, supercapacitors and lithium ion batteries [8–10].

Recently, a novel class of 2DMs entitled as "MXene" has been discovered with similar properties as that of other 2DMs. MXenes are categorized as early transition metal carbides and nitrides. MXenes are obtained by etching and chemical exfoliation of layered carbides in MAX phases, where M is the early transition metal, A is the IIIA and IVA group elements such as aluminum (Al) or silicon (Si) and X represents carbon or nitrogen atom and the suffix "ene" represents their similarity with that of graphene. The general formula used for MXene is $M_{n+1}AX_n$ where n ranges from 1 to 3 [11–13]. The first ever MXene material "named as $Ti_3C_2T_z$" was synthesized in 2011 by heating Ti_3AlC_2 in hydrofluoric acid at room temperature [14]. During this process, aluminum atoms are substituted by oxygen atoms, hydroxyl ions or fluorine atoms. The removal of aluminum layer effects the bonding strength of $M_{n+1}X_n$ layers and allow them to be separated easily. Due to the removal of Al layer from the MAX phases, the obtained product was termed as MXene due to 2D nature and similar properties as that of graphene such as high electrical conductivity and stability. Figure 1 represent the schematic illustration of MXene elements having single M layer or a mixture of two different M layers.

Here, M can be any element such as Ti, Ta, V, Nb etc. The MXenes studied so far includes V_2CT_x, $Ti_3C_2T_x$, $Ta_4C_3T_x$, $Nb_4C_3T_x$, Ti_2CT_x and Nb_2CT_x, here T_x denote the surface groups such as oxygen, fluorine and hydroxyl ions [16–18]. Some other MXene solutions have also been reported such as Ti_3CNT_x, $(V_{0.5}Cr_{0.5})_3C_2T_x$ and $(Ti_{0.5}Nb_{0.5})_2CT_x$ having thickness less than 1 nm [19, 20].

MXenes have distinctive properties of metallic conductivity and hydrophilic nature which exposed many promising applications in energy conversion and storage devices such as hydrogen evolution reactions, supercapacitors, sodium capacitors, potassium, lithium and sodium ion batteries [21–25]. The discovery and extensive utilization of MXene, extends their potential applications in the development of future nanoelectronics and energy device applications.

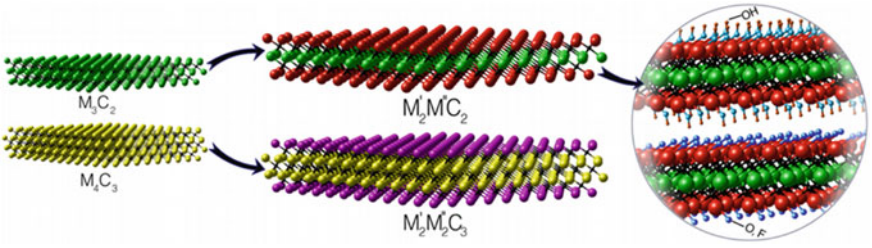

Fig. 1 Schematic of MXenes having single and bilayers of M element [15]

2 Synthesis of MXenes

Generally, two routes are employed for the synthesis of MXene including bottom-up approach and top-down approach. The bottom-up approach utilizes chemical vapor deposition (CVD) technique which is used to synthesize high quality film on a substrate. In most of the cases, the films grown by this method contains stacked multilayers of the material. On the other hand, the second method for the synthesis of MXene is the top-down approach including exfoliation of layered materials. This method is further subdivided into chemical and physical exfoliation. The synthesis technique is clearly understandable by the flowsheet diagram as shown in Fig. 2. Following section summarizes different techniques for the synthesis of MXene.

2.1 Synthesis of MXene by Bottom-Up Approach

In recent years, many bottom-up techniques have been exploited for the synthesis of transition metal nitrides and carbides such as CVD technique [26, 27], plasma enhanced pulsed laser deposition (PELPD) technique and template method [28]. The materials produced by using these techniques exhibits high crystallinity. However, the thin films produced by such methods are not single layer but consists of few thin layers having the similar electronic characteristics as that of other two-dimensional materials.

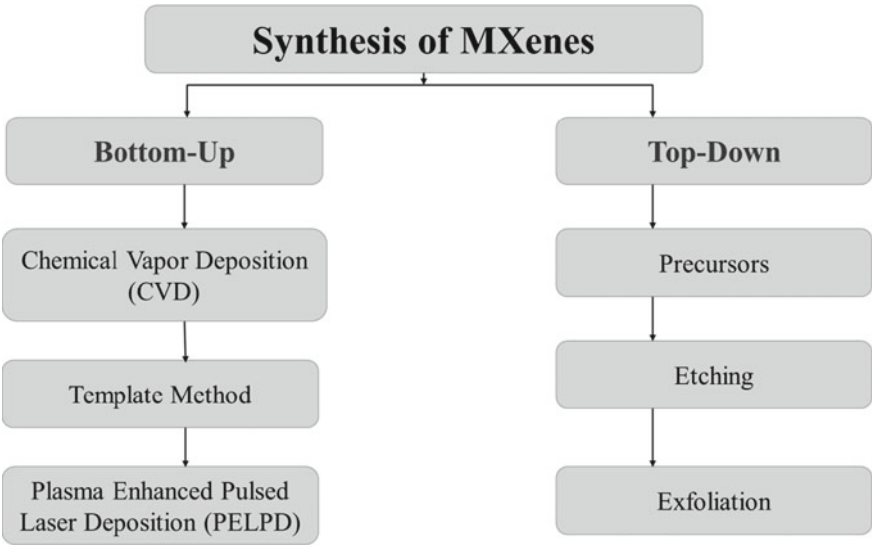

Fig. 2 Flowsheet diagram of synthesis of MXenes dividing in two main categories

Xu et al. was the first to report the synthesis of transition metal carbides crystals by using chemical vapor deposition technique in which copper and transition metal was used as a substrate [29]. The stack of copper and molybdenum foils was preheated at a high temperature of 1085 °C to produce thin films of α-Mo_2C crystals. The crystals were grown on liquid copper surface in the presence of methane and hydrogen. The liquid copper layer exhibits many advantages as it improves the decomposition process of methane by acting as a catalyst and it also provide a channel for controlled diffusion of molybdenum atoms to the liquid copper surface which leads to the formation of Mo_2C crystals on copper surface. Figure 3a is the schematic illustration of Mo_2C crystals that are grown on a Cu and Mo substrate. The as-grown ultrathin crystals of Mo_2C is based on various definite shapes such as rectangles, triangles and hexagons having 3–20 nm thickness. Moreover, after etching of copper by using $(NH_4)_2S_2O_8$, the crystals can easily be transferred on any desired target substrate. It was also observed that Mo atoms consisted of a symmetrical hexagon structure having rotational symmetry with three or six domains except octagon and rectangular crystals [30]. Figure 3b–d illustrate three different domain boundaries which have a strong impact on the conductivity of 2D materials. Further studies showed that the crystal shape of Mo_2C can be transformed from triangular to other polygonal structure by varying the amount of methane flow [31].

Similar to the formation of Mo_2C crystals, Wang et al. reported the growth of tantalum carbide (TaC) crystals by using CVD technique [34]. Ammonia as a source of nitrogen can be used for the synthesis of two-dimensional TaN crystals. In this case,

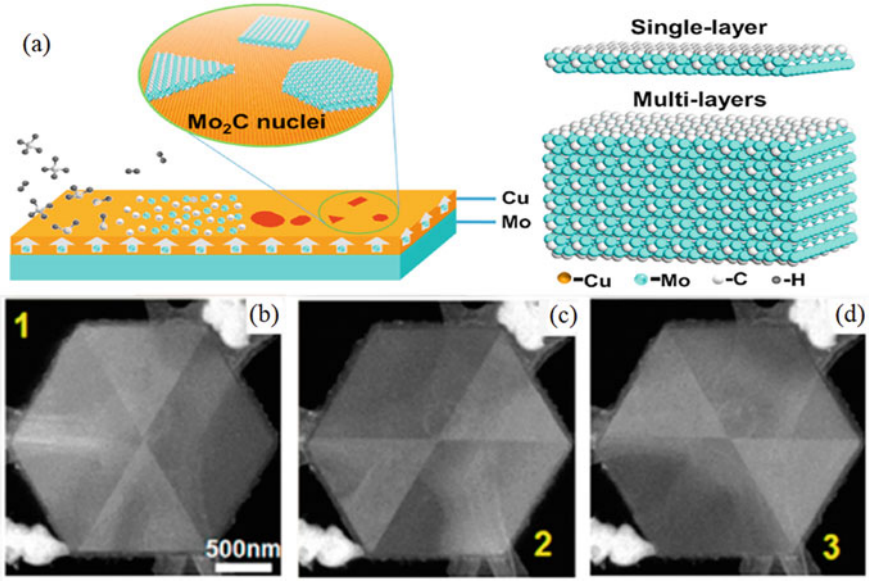

Fig. 3 **a** Schematic illustration of growth of two-dimensional Mo_2C crystals. **b–d** Transmission electron microscopy image indicating well-defined domain structure of Mo_2C crystal [30, 32, 33]

Cu foil at 1077 °C is kept in solid form during the whole procedure. Moreover, DFT calculations prove that the thickness of two-dimensional crystals can be controlled easily at lower temperature. The temperature below the melting point of Cu is sufficient to supply energy to Ta atoms to fill the vacant sites of Cu lattice. Just similar to transition metal carbides and nitrides, CVD method is also utilized for the synthesis of transition metal chalcogenides [35]. Previous reports demonstrate two-different methods to grow two-dimensional vertical heterostructures of Mo_2C and graphene. One method is the direct-step CVD in which methane was used in higher concentration for the formation of graphene [35]. Second method is two-step CVD in which graphene was initially grown on Cu substrate at low temperature (below melting point of copper) and then temperature was gradually raised to grow Mo_2C crystals under the graphene layer [36]. Figure 4a shows the schematic illustration of two-step method of using CVD to develop vertical heterostructures of Mo_2C/graphene. The crystals obtained by using two-step method exhibits high crystallinity and non-uniform strain domains which results in super conductive behavior.

Another technique used in the bottom-up approach is the template method in which two-dimensional transition metal oxides are utilized as a template which is further carbonized to form transition metal carbides [37, 38]. Xiao et al. discussed the formation of MoN nanosheets by using MoO_3 as a template forming a hexagonal structure as shown in Fig. 4b. The resulted nanosheets of MoN are uniform having a thickness of 0.71 nm as observed by using HR-TEM image in Fig. 4c. In another studies, MoN nanosheets are synthesized by using template method in which Mo filament treated with oxygen is used as a template nanosheets of MoO_3 are vertically

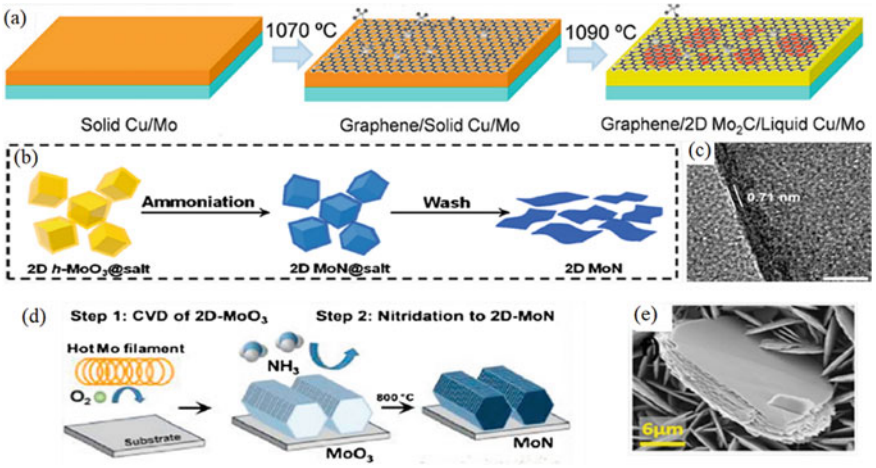

Fig. 4 **a** Schematic demonstration of two step CVD of two-dimensional Mo_2C/graphene heterostructure [36], **b** Schematic view of template method for synthesizing MoN nanosheets [37].**c** HRTEM image representing edge view of MoN nanosheets. **d** Schematic demonstration of template assisted process of ultrathin MoN nanosheets. **e** SEM image of vertically aligned MoN nanosheets grown on a FTO substrate [38]

grown over it [38]. Two-dimensional MoO_3 nanosheets was then heated at 800 °C in the presence of ammonia which transformed MoO_3 into MoN nanosheets resulting in a layered structure having 20–30 μm lateral size and thickness of about 5–40 nm as illustrated in Fig. 4d, e.

Another bottom-up approach is the PELPD, which is recently reported by Zhang et al. for synthesis of ultrathin Mo_2C FCC films on sapphire substrate [39, 40]. To deposit high quality films of Mo_2C, the substrate was heated at 700 °C by using methane plasma as carbon source followed by the generation of Mo vapor by pulsed laser. The resulting films possessed a thickness of 2–25 nm with low crystallinity as compared to CVD-grown nanosheets.

2.2 Synthesis by Top-Down Approach

Since the exploration of first MXene, $Ti_3C_2T_z$ family grew so fast that up till now more than 30 different arrangements have been designed by using precursor and etching processes. Following section will discuss different top-down approaches to synthesize MXene.

The MAX phases comprised of more than 130 different compositions having octahedral structure [41]. Three types of MAX phases have been reported such as 211, 312 and 413 having 1, 2 and 3 number of M layers between A layers, respectively. Over 30 different MXenes are obtained from aluminum containing MAX phases by etching aluminum. Some new layered solids such as $(MC)_n(AlSi)_4C_3$ and $(MC)_n(Al_3C_2)$ are recently reported as precursors which are etched to form $Hf_3C_2T_z$ and $Zr_3C_2T_z$, respectively [42, 43]. The structural or chemical order in MXenes is of profound significance and is directly related to the parent's phase order. Recently, two types of MAX phases are explored having phases 312 and 413 which is titled as out-of-plane ordered and another one comprises of 211 phase which is labeled as in-plane ordered MAX phases [44, 45]. For out-of-plane ordered quaternary MAX phases, one layer of M element which is either monolayer or double layer is sandwiched between another layer of M element such as $(Mo_{2/3}Ti_{1/3})_3AlC_2$ and $(Mo_{2/3}Sc_{1/3})_3AlC_2$ in which Mo is the front layer and Ti and Sc are the inner layers. More than 11 molybdenum based MAX phases have been recently exploited.

For the transformation of MAX phases to MXenes, different termination groups such as fluorine, oxygen or hydroxyl are used in place of etched layers. After etching, the obtained material is based on multilayers which are bonded together by hydrogen or van der Waal bonds. Ternary MAX phase element Ti_3AlC_2 can be converted to $Ti_3C_2T_z$ by adopting different etching techniques [14]. Among those techniques, one method is comprised of mixing Ti_3AlC_2 powder in hydrofluoric acid where bonds between M-A and M-X reacts with hydrofluoric acid resulting in the selective etching of aluminum layers. Etching condition depends on the structural order of MAX phases of parent element. Due to the corrosive and hazardous behavior of hydrofluoric acid (HF) a different route has been exploited to avoid the use of HF by replacing it with the mixture of hydrochloric acid (HCl) and fluoride salt [46]. Some

other fluoride salts are sodium fluoride (NaF) and potassium fluoride (KF) which can be mixed with HCl and can be utilized instead of HF [47, 48]. Ammonium hydrogen bifluoride was also reported as a good contender to replace HF for the etching of Al from Ti_3AlC_2. Mostly, the element etched from MAX phases was aluminum but recently silicon (Si) was also etched from its MAX phase Ti_3SiC_2 by using HF as an oxidant [49].

After etching process, next step is to exfoliate the etched layers for obtaining few or multilayers of MXenes. But before exfoliation, the etched layers are frequently washed with distilled water to remove the residues of etching solution. Prewashing with sulphuric acid (H_2SO_4) and HCl is also helpful in dissolving the residual salts such as AlF_3 and LiF [50]. After washing the etched layers, different exfoliation methods such as direct sonication or liquid exfoliation can be adopted to obtain MXene layers. Direct sonication results in low yield of MXenes as compared to liquid exfoliation which gives higher yield up to 20 mg per mL solution. Different organic molecules such as dimethyl sulfoxide (DMSO) [51], iso-propylamine [52], tetra butyl ammonium hydroxide (TBAOH) [53], choline hydroxide and n-butylamine are used to carried out exfoliation of $Ti_3C_2T_z$, $(Mo_{2/3}Ti_{1/3})_3C_2T_z$, Ti_3CNT_z and V_2CT_z, respectively [54]. Figure 5a is the schematic representation of the preparation of MXene sheets by using top-down approach. MXenes obtained from the top-down approach exhibits some significant characteristics such as the chemical order in i- and o-MAX phases which does not deteriorate by the etching of Al. Some of the MXene elements that are obtained from o-MAX phase parent elements having Ti in the inner layers are $(Cr_{2/3}Ti_{1/3})_3C_2T_z$, $(Mo_{1/2}Ti_{1/2})_4C_3T_z$ and $(Mo_{2/3}Ti_{1/3})_3C_2T_z$ [12,

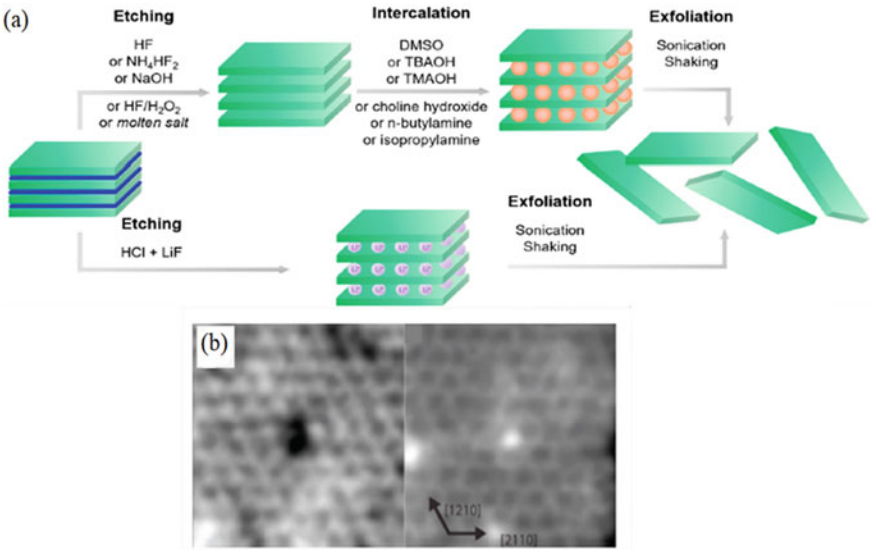

Fig. 5 **a** Schematic illustration of synthesizing MXene by top-down approach. **b** HRTEM image of $Ti_3C_2T_x$ showing atomic defects in single layer MXene [32]

55]. The inner layers play an important role towards the stability of the molecule during etching process. The etching and exfoliation of $Ti_3C_2T_z$ may arise some defects at atomic scale which are observed by transmission electron microscopy (TEM) as shown in Fig. 5b. It was observed that by enhancing the concentration of HF during etching ultimately increases the amount of defects. At microscopic level, some defects are observed in single layer of MXene which also depends on etching environments. One major drawback of conducting exfoliation by sonication is the excessive increase in the number of pores in Mo_2CT_z.

Recently, more than 30 different compositions of MXenes have been synthesized by using top-down approach and DFT calculations predict the existence of many more. New elements of MXene family and new etching processes are being discovered with time.

3 Properties of MXenes

3.1 Structural Properties

The novel 2D material, MXene, exhibits unique structural properties such as hydrophilic nature and active edge sites which enhance its significance in many practical applications. In a recent study, the geometry of Ti_2C and Ti_3C_2 MXene was optimized by adding methoxy functional group [56]. The lattice parameters are found to be 3.3338 and 3.2921 A^o which is in good agreement with the theoretical estimation. The lattice parameters of $Ti_2C(OH)_2$ and $Ti_3C_2(OH)_2$ strongly depends upon the type of hydroxyl ion covering. It was observed that partially and fully covered methoxy or hydroxyl group increases the lattice parameters. Figure 6a demonstrate the dependence of Ti_2C and Ti_3C_2 lattice parameters with the functionalization groups such as AA, BB and AB. In further studies, tailoring the structure of

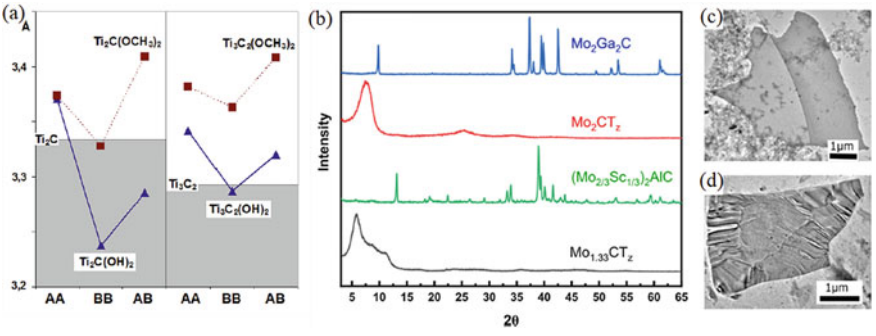

Fig. 6 **a** Optimation of lattice parameters for Ti_2C and Ti_3C_2 by varying surface covering of functionalized groups. **b** X-Ray diffraction pattern of various molybdenum based MXenes. **c**, **d** TEM images of Mo_2CT_x and $Mo_{1.33}CT_z$, respectively [56, 58]

MXene was investigated by adopting different etching protocols such as the transformation of i-MAX phase of $(Mo_{2/3}Y_{1/3})_2AlC$ into in-plane order $(Mo_{2/3}Y_{1/3})_2C$ and in-plane vacancy order (Mo1.33C) [57]. Electrochemical investigations reveal different results for both in-plane order element and in-plane vacancy order and it was observed that vacancy ordered MXene show relatively good results.

The atomic surface structure of MXene plays an important role in the electrocatalytic activity towards hydrogen evolution reaction (HER). Intikhab et al. synthesized $Mo_{1.33}CT_z$ and Mo_2CT_z to study the electrochemical behavior of these MXenes towards HER [58]. Results indicate that the in-plane ordered vacancy in $Mo_{1.33}CT_z$ causes to decrease the HER comparative to Mo_2CT_z. Figure 6b represents the XRD pattern of the parent's MAX phases and their corresponding MXenes. No peak was found at 61° which confirms that the large number of flakes parallel to the substrate belongs to the 110 family of planes. TEM images (Fig. 6c, d) show that Mo_2CT_z and $Mo_{1.33}CT_z$ includes single and multilayers. The catalytic activity is attributed to the basal planes which are confirmed by the orientation with respect to the substrate. It can be concluded that the structural arrangement of MXene is directly linked with the catalytic performance. Furthermore, Shuck et al. investigate the structural properties of $Ti_3C_2T_z$ MXene by their synthesis from graphite, carbon lampblack and titanium carbide and discuss the electrical conductivity and stability of these MXenes [59]. The obtained products contain the flakes of different sizes, composition, stability and conductivity. MXenes derived from graphite exhibits the highest stability and electrical conductivity as compared to titanium carbide and carbon lampblack derived MXenes.

3.2 Electrical and Magnetic Properties

Khazaei et al. investigated fabricated and investigated the electrical properties of various MXene types such as M_2C and M_2N where M is Sc, Ti, Zr, Cr, V along with some functional group such as F, O and OH [60]. It was evidenced that attachment of suitable functional group e.g. Ti_2C, Hf_2C, Sc_2C and Zr_2C MXenes show semiconducting behavior. Some theoretical studies ensure that Cr_2C and Cr_2N show magnetic behavior. Results reveal that MXenes show metallic as well as superconducting behavior. It is inferred theoretically that the $Sc_2C(OH)_2$ exhibits a direct band gap whereas other semiconductors possess an indirect band gap. The electronic properties of MXenes are affected by the type of functional group attached with it. For instance, F and OH functional groups can alter the electrical properties by receiving one electron from the surface whereas O group need two electrons to get stable. Pure MXenes show metallic behavior as their Fermi energy is in d band of the transition metals whereas some MXenes have p band below that of the d band having a small band gap between both bands. It was also found that transition metals show low electronegativity due to which these transition metals donate electrons to other atoms and itself becomes positively charged. Due to the magnetic nature of chromium compounds, spin polarized PBE method reveals that ground states

of chromium carbide and chromium nitride show ferromagnetic behavior whereas other functionalized MXenes show nonmagnetic behavior. The magnetic properties of Cr_2C and Cr_2N can be tailored by applying strain. Figure 7a represents the resistivity versus temperature curves for Ti based films. Ti based films demonstrate the metallic behavior with the linear enhancement in resistivity with respect to temperature. It was observed that below 50 K temperature the decreasing resistivity attribute to the weak localization in this metallic behavior. The results were matched with the previous studies where $Ti_3C_2T_x$ was synthesized from sputter deposited epitaxial films in which the as-synthesized MXene show metallic response at high temperature and weak localization at low temperature. Magnetoresistance is also plotted in Fig. 7b at 10 K temperature. The negative magnetoresistance for Ti based films indicate that as-synthesized MXene is etched in hydrofluoric acid or ammonium hydrofluoride and also confirms the weak localization. Moreover, Miranda et al. investigated the electrical properties of monolayer $Ti_3C_2T_x$ MXene [61]. Results reveal the metallic nature of $Ti_3C_2T_x$ MXene in which carrier density can be altered by varying gate voltages. In the presence of magnetic field, electrical transport measurements show a quadratic increase in the conductance. It can be observed from field effect measurements that at backgate voltage of 18 V there occurs an abrupt change in the conductance slope. At region below 18 V charge carrier mobility is found to be 0.2 cm^2/Vs whereas in region where gate voltage is greater than 18 V the mobility is 0.8 cm^2/Vs. The study indicates that $Ti_3C_2T_x$ MXene exhibits potential applications in transparent conductive films. The metallic nature of $Ti_3C_2T_x$ is very favorable for superconductor applications.

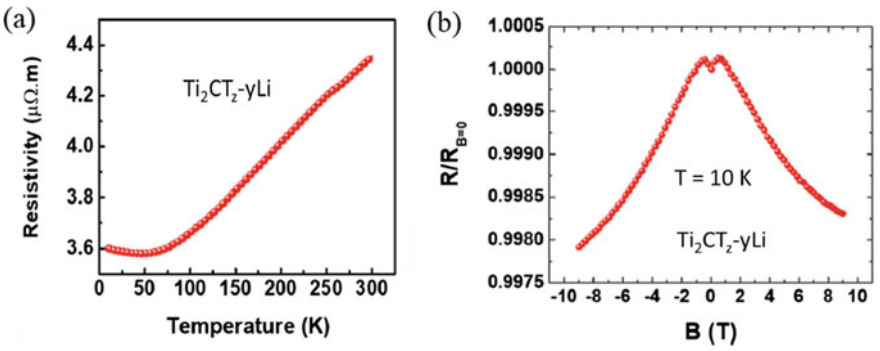

Fig. 7 **a** Temperature dependent resistivity measurement of Ti2CTz-yLi nanosheets. **b** Magnetoresistive curve of Ti2CTz-yLi film [62]

3.3 Optical and Charge Transport Properties

The optoelectronic properties of early discovered MXene ($Ti_3C_2T_z$) was investigated by spray coating its colloidal solution to fabricate conductive thin films [17]. The evaluation of optical properties of $Ti_3C_2T_z$ was studied by using UV-VIS spectrophotometry. Light is absorbed by the films in ultraviolet region and it was evidenced that absorption peak at 270 nm corresponds to glassy substrate whereas band in the range of 700–800 nm represents pale greenish color. In the visible region these films show a flat absorption response due to which these films can be used for display applications. It was also observed that by increasing the film thickness the transmittance lowers down while at about 70 nm the transmittance is retained about 43.8%. About 40–90% transmittance is most suitable for transparent conductive applications Along with good optoelectronic properties $Ti_3C_2T_z$ possesses good mechanical properties as well. The sheets were folded on a flexible substrate and sheet resistance was measured as function of bending radii. During measurements the sheets were held folded for about 5 min and after removing stress the sheets were recovered immediately showing an excellent mechanical stability. As various MXene types exhibit an indirect band gap which limits their utilization in optoelectronic devices. However, the issue can be resolved by transforming an indirect band gap to the direct band gap by applying tensile strength. The transition from indirect to direct band gap can be performed by different structures and functional groups. Further studies referred that semiconducting MXenes show better stability towards biaxial strain and have the capability to maintain their stability for excessive strain [63]. The unique structural, electromagnetic, optoelectronic and mechanical properties of MXenes makes it a promising material for many practical applications.

Owing to high mobility and suitable band gap of two-dimensional materials, Lai et al. investigate the electrical transport properties of Ti_2CT_x MXene field-effect transistors by varying the surface functional groups such as F, O and OH through different synthesis techniques [64]. Results indicate that Ti_2CT_x demonstrate a high mobility of 10^4 cm^2/Vs at room temperature and temperature dependent study reveals the superconducting behavior of Ti_2CT_x. Results confirm better electric charge transport property of MXene by optimizing the treatment methods.

4 Applications of MXenes

MXenes show potential applications in various field of research such as energy conversion and storage systems, electrocatalytic reactions such as hydrogen evolution reaction (HER) and oxygen reduction reaction (ORR) and in the field of biomedical research. Different applications of MXenes based on their structural and optoelectronic properties are discussed as follows.

4.1 Biomedical Applications of MXenes

The attractive physiochemical properties of MXenes makes them a promising candidate in different biomedical applications such as biosensors, bio-imaging, antibacterial activity and drug delivery systems [65–69]. Xue et al. synthesized Ti_3C_2 quantum dots (MQDs) by using a hydrothermal technique and investigate their bio-imaging applications [70]. The prepared MQDs can be attributed to quantum confinement due to hydrothermal process and the size of MQDs can be changed by tailoring the reaction temperature. The uniformity in the nanoscale size of MQDs allow them to penetrate through the cells and have potential applications in bio-imaging. Similar work was done by Zhou and his coworkers, who synthesized $Ti_3C_2T_x$ Mxene QDs in dimethyl-formamide (DMF) and explored their potential in cell-imaging [71]. Besides cell-imaging, MXenes can also be used in computed tomography (CT), magnetic resonance (MR) and photo-acoustic (PA) imaging. Ta_4C_3 MXene having tantalum element makes it more suitable for CT imaging due to high atomic number [66, 72].

In the current age, cancer is the most lethal disease and different therapeutic strategies have been adopted to destroy cancer cells. Among those strategies, chemotherapy, radiotherapy and photothermal therapy is mostly common [73]. In photothermal therapy, light is transformed to the cancer sites and restrict the growth of tumor cells [74]. MXenes have high absorption and facilitate in the photo thermal-conversion efficiency (PCE). Lin et al. utilized Nb2C MXene as a highly efficient photo thermal agent in photo thermal extirpation of mouse tumor. In contrast to PTT, chemotherapy not only deteriorates the cancer cells but also cause damage to normal tissues. Therefore, an effective and controllable drug delivery system should be designed to reduce the harm to normal tissues. MXenes have prolific advantages in providing drug delivery channels due to its large surface area. Recently discovered MXene (Ta_4C_3) are used as X-Ray CT contrast agent [75]. Another potential application of MXenes is found in antibacterial activity such as photodynamic therapy (PDT) for killing cells [68]. A conducting bridge is placed over an insulating lipid bilayer which facilitates the transfer of electrons from intercellular components to the environment and cause the death of cells.

4.2 Energy Storage Applications

Electrochemical energy storage devices are a clean source to store renewable energy. Variety of two-dimensional materials (carbon, fullerene, graphene, carbon nanotubes etc.) are used in energy storage applications due to their admirable characteristics such as high mechanical strength, large surface area and high electrical conductivity [76–78]. Similarly, MXenes also show promising applications in energy conversion and storage devices such as photoelectrochemical cell (PEC), supercapacitors, lithium ion batteries, electro-catalysts and sodium ion batteries [70, 79, 80]. The

hydrophilic nature of MXene suggests it a powerful candidate for the photo-anodes in photoelectrochemical water splitting in which incident photons strike the surface of photo-anode to liberate electrons and holes which individually react with OH^- and H^+ to form water and hydrogen. Yu et al. synthesized Ti_3C_2 nanoparticles to synthesize a metal oxide/MXene heterostructure and use the heterostructure for photo-anode in photoelectrochemical water splitting [81]. A significant increase in the photoconductivity and stability is observed for the as-synthesized heterostructure. Furthermore, Chen et al. fabricated inverse opal photonic crystals of titania and Ti_3C_2 quantum dots heterostructure [82]. Titania enables efficient charge separation and thus enhances the charge transportation resulting in an increase in photoconductivity of PEC based sensor. Bismuth vanadate was also utilized as photo-anode in PEC water oxidation. Due to lack of charge transport and slow kinetics in bismuth vanadate, Yan et al. synthesized MXene flakes on the surface of $BiVO_4$ grown on a fluorine doped tin oxide substrate [83]. The as-prepared composite of Ti_3C_2/Mxene reveals a remarkable increase in the photocurrent density up to approximately 3 $mAcm^{-2}$ and photo-conversion efficiency up to 0.78%. The coating of Ti_3C_2 on the surface of $BiVO_4$ facilitates in the efficient charge separation and reduce the recombination of photo-generated electrons and holes due to unique anisotropic structure. The photoelectrochemical properties of as-prepared composite was investigated in three electrode cell configuration with 1 M solution of potassium borate. All results of photoelectrochemical measurements are demonstrated in Fig. 6. J-V curves show a higher photocurrent density of 3.45 $mAcm^{-2}$ for Ti_3C_2/MXene composite and a higher efficiency of 0.78% as shown in Fig. 8a, b. The electrochemical stability of the as-prepared composite was also studied by using chronoamperometry measurements as illustrated in Fig. 8c. Results reveal that $Ti_3C_2/BiVO_4$ composite is more stable as compared to pristine $BiVO_4$. Ti_3C_2 (MXene) causes to enhance the photoconductivity and improves the photocatalytic activity of $BiVO_4$ as well.

Furthermore, MXenes play an important role in energy storage devices such as supercapacitors and batteries. Supercapacitors are divided into three types which includes electric double layer capacitor, pseudocapacitor and hybrid supercapacitors. Supercapacitors have more power density and quick charge/discharge rate while in contrast the batteries have large energy density and high specific capacities [84]. Carbon based materials are found very effective as electrode materials for energy storage systems. Carbonaceous materials such as activated carbons, graphene, fullerene, carbon nanotubes etc. are employed for electrode materials in supercapacitors [85–87]. Similarly, the emerging class of two-dimensional material MXene is also frequently used in supercapacitor applications due to its layered MAX phases and remarkable electrical properties. In supercapacitors charge stores at electrode/electrolyte interface through physical adsorption. The fast charging discharging capability of supercapacitors and long cyclic durability enhance its utilization in vehicles and power stations. In one studies, the etching of aluminum from T_3AlC_3 results in the synthesis of tantalum carbide Ta_4C_3 which was electrochemically tested for supercapacitor electrode in 0.1 M H_2SO_4 electrolyte [88]. From structural analysis it was found that Ta_4C_3 exhibits a hexagonal lattice structure and electrochemical analysis reveals better performance of as-synthesized electrode material in energy

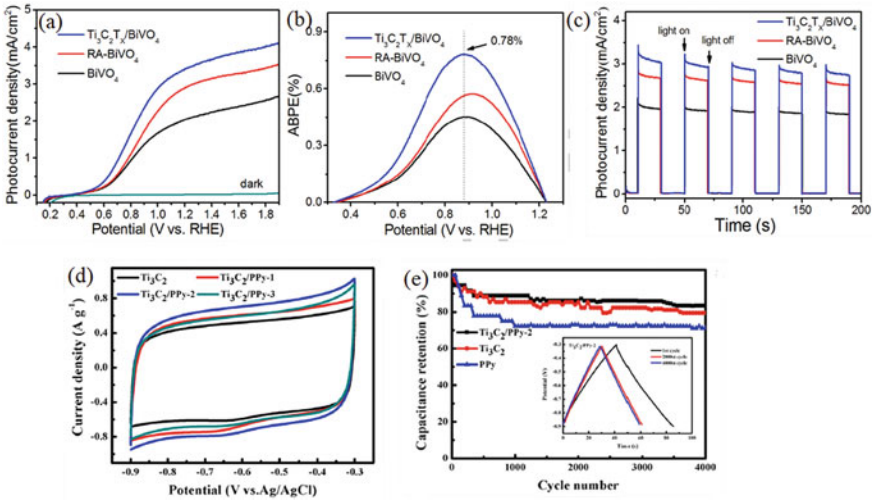

Fig. 8 **a** Linear sweep voltammetry measurements of $BiVO_4$, RA-$BiVO_4$ and $Ti_3C_2T_x/BiVO_4$ photoanodes. **b** Applied bias photon to current conversion efficiency of $BiVO_4$, RA-$BiVO_4$ and $Ti_3C_2T_x/BiVO_4$ photoanodes for PEC water splitting. **c** Chronoamperometry measurements of $BiVO_4$, RA-$BiVO_4$ and $Ti_3C_2T_x/BiVO_4$ photoanodes under1.23 v versus RHE [83]. **d** Cyclic voltammetry measurements of Ti_3C_2 and Ti_3C_2/ppy composites at 10 mV/s scan rate. **e** Cyclic stability test of Ti_3C_2/ppy-2, Ti_3C_2 and ppy electrodes for 4000 cycles at 1 A/g [89]

storage applications. The estimated specific capacitance was found to be 481 F/g with a cyclic retention of about 89% after 2000 cycles of continuous charge/discharge. Furthermore, the selective etching of Al from V_4AlC_3 results in multilayered V_4C_3 MXene which show a gravimetric capacitance of 209 F/g with a cyclic retention of about 97% after 10,000 cycles. The factors which contribute in high capacitance is wide interlayer spacing approximately 0.466 nm, pore volume of about 0.047 cm^3/g, good hydrophilicity and large surface area of about 31.35 m^2/g. Similarly, further studies suggest that dispersed nanoparticles of polypyrrole (ppy) on Ti_3C_2 nanosheets may act as a promising material for supercapacitor electrodes [89]. Electrochemical tests were performed in three electrode assembly by using platinum plate as a counter electrode, Ag/AgCl as reference electrode and Ti_3C_2/ppy nanocomposite as working electrode and Na_2SO_4 as electrolyte. The cyclic voltammetry curves show a specific capacitance of approximately 184 F/g at scan rate of 2 mV/s with a cyclic stability of 83.33% after 4000 cycles as shown in Fig. 6d, e. The addition of polypyrrole expand the interlayer spacing of Ti_3C_2 MXene which facilitates in the ion and charge transportation. The electrochemical behavior of nanocomposite is improved due to the synergistic effect of both MXene and polypyrrole.

Similar to supercapacitors, MXenes are also employed for anode material in rechargeable batteries such as (Li, K, Na) ion batteries due to their dominant characteristics [90]. In case of Li ion batteries, Li act as electron donor (anode) and lithium cobalt oxide as electron acceptor (cathode) separated by an ionic electrolyte. Initially,

reduction reaction occurs at cathode liberating lithium ions during charging whereas in discharging process, lithium ions releases from anode and move towards cathode. Intercalation process took place during charging whereas deintercalation process occur during discharging of lithium ion batteries. Due to continuous shuttling of lithium ions from anode to cathode such types of cells are also known as rocking chair cells. MXenes play a crucial role in secondary batteries due to the dominant structural and electrical properties. Variety of MXenes such as V_2C, Ti_2C, Sc_2C and Nb_2C are theoretically estimated to have high specific capacities as compared to M_3X_2 and M_4X_3. Sun et al. has synthesized Ti_3C_2 through exfoliation of Ti_3AlC_2 and use Ti_3C_2 as anode for lithium ion batteries [91]. Electrochemical analysis reveals a high capacity of 123.6 mAh/g having a columbic efficiency of about 47%. The volumetric capacitance of Li ion battery is a major issue which restrict its practical applications such as electric vehicles. To overcome this limitation, Wang et al. fabricated a MXene hybrid of $Fe_3O_4@Ti_3C_2$ by using ultrasonication process [92]. Electrochemical performance of as-prepared MXene hybrid was evaluated by using a coin cell type geometry. The CV curves of MXene hybrid was obtained at a scan rate of 0.2 mV/s. Broad reduction peaks were found for Ti_3C_2 at a potential of 0.67 V and 0.28 V whereas a strong reduction peak at a potential of 0.69 V was found for pristine Fe_3O_4 and $Fe_3O_4@Ti_3C_2$ MXene hybrid. The CV results show a high reversible specific capacity of about 747.4 mAh/g for $Fe_3O_4@Ti_3C_2$-2.5 sample. The cyclic durability of the abovementioned sample was electrochemically studied. Results reveal a good cyclic performance of $Fe_3O_4@Ti_3C_2$ MXene. In this case, the obtained volumetric capacitance was 2038 mAh/g. Therefore, it can be concluded that such type of hybrid MXenes are promising anode materials for energy storage devices.

Along with exceptional characteristics of electrode and anode in energy storage devices, MXenes also exhibit dominant features as a catalyst in hydrogen evolution reaction (HER). Among various two-dimensional materials MoS_2 has been widely explored for different electrocatalytic applications and theoretical studies confirm that edge sites are responsible for all catalytic activities. Therefore, to improve the efficiency of HER it is necessary to enhance the exposure of edge sites. Due to similar characteristics of MXenes as other two-dimensional materials, it is also considered to possess good catalytic performance. In this regard, Seh et al. reported the application of MXenes as an effective electrocatalyst for the very first time [93]. Both theoretical and experimental studies were analyzed to predict MXene as an active catalyst for HER. Initially, Mo_2CT_x and Ti_2CT_x was theoretically studied and it was found that Mo_2CT_x exhibit higher catalytic activity in HER as compared to Ti_2CT_x. Basal planes of Mo_2CT_x are electrocatalytically more active towards HER as compared to MoS_2. Density functional theory (DFT) calculations estimates that Mo_2CT_x have less Gibbs energy which confirms its higher HER performance. Along with theoretical studies, experimental analysis was also performed to investigate the catalytic performance and stability of MXenes. For experimental studies, Mo_2CT_x and Ti_2CT_x was etched from Mo_2Ga_2C and Ti_2AlC by using hydrofluoric acid. The synthesis results in the attachment of functional group (T_x) on basal planes of MXenes. Linear sweep voltammetry measurements were conducted as shown in

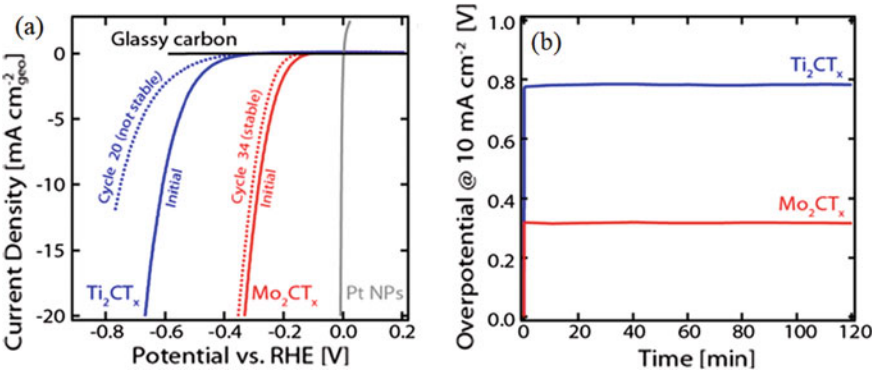

Fig. 9 **a** Linear sweep voltammograms of Mo_2CT_x and Ti_2CT_x compared with bare glassy carbon electrode. **b** Chronopotentiometry measurement of Mo_2CT_x and Ti_2CT_x at a constant current density of 10 mA/cm^2 [93]

Fig. 9a to investigate the catalytic activity of as-synthesized MXenes towards HER. It was observed that catalytic activity of Ti_2CT_x is continuously decreasing showing the unstable nature of Ti_2CT_x whereas Mo_2CT_x demonstrate comparatively a higher HER activity with a slight decrease upon continuous cycling indicating more stability of Mo_2CT_x. The stability of both MXenes were evaluated at a constant current density of 10 mA/cm2 as plotted in Fig. 9b and results reveal no substantial change in the overpotential of Mo_2CT_x and Ti_2CT_x. However, after conducting stability measurement, both MXenes were again tested by LSV which shows that HER activity of Ti_2CT_x was further decreased. In short, both theoretical and experimental studies verify a remarkable HER performance of Mo_2CT_x which opens the doorway for the development of other two-dimensional materials with excessive active basal planes.

Following table illustrate the comparison of different electrode materials and their corresponding properties in supercapacitors and lithium ion batteries (Table 1).

5 Conclusion

In summary, a new class of two-dimensional materials based on early transition metal carbides and nitrides are explored which can be synthesized by etching A element from MAX phases along with the attachment of surface functional groups such as OH, F and O. The term MXene emphasize on their two-dimensional structure and highlights the loss of Al (A element) from its MAX phase. Up to date, numerous MXene elements have been exploited such as Ta_4C_3, Ti_2C, V_2C, Nb_2C, NB_4C_3 etc. Many new elements have been theoretically predicted. Various synthesis process results in the formation of multilayered flakes such as sonication process. Therefore, to obtain a single thin layer of MXene some new synthesis techniques are required. The 2D morphology and high electronic conductivity of MXenes makes

Table 1 Comparative analysis of various two-dimensional materials based electrodes for supercapacitor and lithium ion batteries

Electrode materials	Specific capacitance (F/g)	Current density (A/g)/scan rate	Electrolytes	References
Reduced graphene oxide/carbon black	79	1	H_2SO_4	[94]
rGO/MWCNTs/polypyrrole	82	0.5	KCl	[95]
CNT/Mn_3O_4/Graphene	73	0.5	KCl	[96]
Graphene hydrogel	186	1	H_2SO_4	[97]
Graphene/PANI	210	0.3	H_2SO_4	[98]
$Ti_3C_2T_x$/carbon nano fibers	70 mF/cm^2	50 mV/s	H_2SO_4	[99]
Two dimensional titanium carbide	520 mF/cm^2	2 mV/s	KOH	[100]
Ti_2CT_x	180 mAh/g	20 mA/g	Na+aqueous electrolyte	[101]
Ti_2CT_x	51	1	KOH	[79]
V_4C_3	209	50 mV/s	H_2SO_4	[102]

them promising materials for practical applications such as in supercapacitors and lithium ion batteries. The most frequently used MXene for supercapacitor electrode is Ti_3C_2 due to its electrochemically stable nature. The excessive edge sites marked MXenes as useful candidate for electrocatalyst in HER activity. Many experimental and theoretical studies such as DFT calculations are currently employing to explore new MXene elements with extraordinary properties and potential applications.

References

1. Novoselov, K.S., et al.: Electric field effect in atomically thin carbon films. Science **306**(5696), 666–669 (2004)
2. Watanabe, K., Taniguchi, T., Kanda, H.: Direct-bandgap properties and evidence for ultraviolet lasing of hexagonal boron nitride single crystal. Nat. Mater. **3**(6), 404 (2004)
3. Lalmi, B., et al.: Epitaxial growth of a silicene sheet. Appl. Phys. Lett. **97**(22), 223109 (2010)
4. Kamal, C., Ezawa, M.: Arsenene: two-dimensional buckled and puckered honeycomb arsenic systems. Phys. Rev. B **91**(8), 085423 (2015)
5. Ni, Z., et al.: Tunable bandgap in silicene and germanene. Nano Lett. **12**(1), 113–118 (2011)
6. Aktürk, E., Aktürk, O.Ü., Ciraci, S.: Single and bilayer bismuthene: stability at high temperature and mechanical and electronic properties. Phys. Rev. B **94**(1), 014115 (2016)
7. Wang, Q.H., et al.: Electronics and optoelectronics of two-dimensional transition metal dichalcogenides. Nat. Nanotechnol. **7**(11), 699 (2012)
8. Fiori, G., et al.: Electronics based on two-dimensional materials. Nat. Nanotechnol. **9**(10), 768 (2014)

9. Rao, C., Gopalakrishnan, K., Maitra, U.: Comparative study of potential applications of graphene, MoS2, and other two-dimensional materials in energy devices, sensors, and related areas. ACS Appl. Mater. Interfaces **7**(15), 7809–7832 (2015)
10. Wang, X., et al.: Quantum dots derived from two-dimensional materials and their applications for catalysis and energy. Chem. Soc. Rev. **45**(8), 2239–2262 (2016)
11. Naguib, M., et al.: 25th anniversary article: MXenes: a new family of two-dimensional materials. Adv. Mater. **26**(7), 992–1005 (2014)
12. Anasori, B., et al.: Two-dimensional, ordered, double transition metals carbides (MXenes). ACS Nano **9**(10), 9507–9516 (2015)
13. Ng, V.M.H., et al.: Recent progress in layered transition metal carbides and/or nitrides (MXenes) and their composites: synthesis and applications. J. Mater. Chem. A **5**(7), 3039–3068 (2017)
14. Naguib, M., et al.: Two-dimensional nanocrystals produced by exfoliation of Ti3AlC2. Adv. Mater. **23**(37), 4248–4253 (2011)
15. Zhang, C., et al.: Two-dimensional MXenes for lithium-sulfur batteries. InfoMat **2**(4), 613–638 (2020)
16. Ying, G., et al.: Conductive transparent V2CTx (MXene) films. FlatChem **8**, 25–30 (2018)
17. Hantanasirisakul, K., et al.: Fabrication of Ti3C2Tx MXene transparent thin films with tunable optoelectronic properties. Adv. Electron. Mater. **2**(6), 1600050 (2016)
18. Eklund, P., Rosen, J., Persson, P.O.Å.: Layered ternary M n + 1AX n phases and their 2D derivative MXene: an overview from a thin-film perspective. J. Phys. D Appl. Phys. **50**(11), 113001 (2017)
19. Naguib, M., et al.: Two-dimensional transition metal carbides. ACS Nano **6**(2), 1322–1331 (2012)
20. Naguib, M., et al.: New two-dimensional niobium and vanadium carbides as promising materials for Li-ion batteries. J. Am. Chem. Soc. **135**(43), 15966–15969 (2013)
21. Yan, J., et al.: Flexible MXene/graphene films for ultrafast supercapacitors with outstanding volumetric capacitance. Adv. Func. Mater. **27**(30), 1701264 (2017)
22. Zhu, M., et al.: Highly flexible, freestanding supercapacitor electrode with enhanced performance obtained by hybridizing polypyrrole chains with MXene. Adv. Energy Mater. **6**(21), 1600969 (2016)
23. Dall'Agnese, Y., et al.: Two-dimensional vanadium carbide (MXene) as positive electrode for sodium-ion capacitors. J. Phys. Chem. Lett. **6**(12), 2305–2309 (2015)
24. Naguib, M., et al.: MXene: a promising transition metal carbide anode for lithium-ion batteries. Electrochem. Commun. **16**(1), 61–64 (2012)
25. Gao, G., O'Mullane, A.P., Du, A.: 2D MXenes: a new family of promising catalysts for the hydrogen evolution reaction. ACS Catal. **7**(1), 494–500 (2016)
26. Lee, Y.H., et al.: Synthesis of large-area MoS2 atomic layers with chemical vapor deposition. Adv. Mater. **24**(17), 2320–2325 (2012)
27. Gogotsi, Y.: Chemical vapour deposition: transition metal carbides go 2D. Nat. Mater. **14**(11) (2015)
28. Halim, J., et al.: Synthesis and characterization of 2D molybdenum carbide (MXene). Adv. Func. Mater. **26**(18), 3118–3127 (2016)
29. Xu, C., et al.: Large-area high-quality 2D ultrathin Mo 2 C superconducting crystals. Nat. Mater. **14**(11), 1135 (2015)
30. Liu, Z., et al.: Unique domain structure of two-dimensional α-Mo2C superconducting crystals. Nano Lett. **16**(7), 4243–4250 (2016)
31. Geng, D., et al.: Controlled growth of ultrathin Mo2C superconducting crystals on liquid Cu surface. 2D Mater. **4**, 011012 (2017)
32. Verger, L., et al.: Overview of the synthesis of MXenes and other ultrathin 2D transition metal carbides and nitrides. Curr. Opin. Solid State Mater. Sci. (2019)
33. Qiao, J.-B., et al.: One-step synthesis of van der Waals heterostructures of graphene and two-dimensional superconducting α − M o 2 C. Phys. Rev. B **95**(20), 201403 (2017)

34. Wang, Z., et al.: Metal immiscibility route to synthesis of ultrathin carbides, borides, and nitrides. Adv. Mater. **29**(29), 1700364 (2017)
35. Deng, R., et al.: Graphene/Mo2C heterostructure directly grown by chemical vapor deposition. Chin. Phys. B **26**(6), 067901 (2017)
36. Xu, C., et al.: Strongly coupled high-quality graphene/2D superconducting Mo2C vertical heterostructures with aligned orientation. ACS Nano **11**(6), 5906–5914 (2017)
37. Xiao, X., et al.: Salt-templated synthesis of 2D metallic MoN and other nitrides. ACS Nano **11**(2), 2180–2186 (2017)
38. Joshi, S., et al.: Facile synthesis of large area two-dimensional layers of transition-metal nitride and their use as insertion electrodes. ACS Energy Lett. **2**(6), 1257–1262 (2017)
39. Zhang, F., et al.: Plasma-enhanced pulsed-laser deposition of single-crystalline M o 2 C ultrathin superconducting films. Phys. Rev. Mater. **1**(3), 034002 (2017)
40. Zhang, Z., et al.: Substrate orientation-induced epitaxial growth of face centered cubic Mo 2 C superconductive thin film. J. Mater. Chem. C **5**(41), 10822–10827 (2017)
41. Barsoum, M.W.: MAX Phases: Properties of Machinable Ternary Carbides and Nitrides. Wiley (2013)
42. Zhou, J., et al.: A two-dimensional zirconium carbide by selective etching of Al3C3 from nanolaminated Zr3Al3C5. Angew. Chem. Int. Ed. **55**(16), 5008–5013 (2016)
43. Zhou, J., et al.: Synthesis and electrochemical properties of two-dimensional hafnium carbide. ACS Nano **11**(4), 3841–3850 (2017)
44. Liu, Z., et al.: (Cr 2/3 Ti 1/3) 3 AlC 2 and (Cr 5/8 Ti 3/8) 4 AlC 3: new MAX-phase Compounds in Ti–Cr–Al–C System. J. Am. Ceram. Soc. **97**(1), 67–69 (2014)
45. Anasori, B., et al.: Mo2TiAlC2: a new ordered layered ternary carbide. Scripta Mater. **101**, 5–7 (2015)
46. Lakhe, P., et al.: Process safety analysis for Ti3C2T x MXene synthesis and processing. Ind. Eng. Chem. Res. **58**(4), 1570–1579 (2019)
47. Liu, F., et al.: Preparation of Ti3C2 and Ti2C MXenes by fluoride salts etching and methane adsorptive properties. Appl. Surf. Sci. **416**, 781–789 (2017)
48. Liu, F., et al.: Preparation of high-purity V2C MXene and electrochemical properties as Li-ion batteries. J. Electrochem. Soc. **164**(4), A709–A713 (2017)
49. Halim, J., et al.: Transparent conductive two-dimensional titanium carbide epitaxial thin films. Chem. Mater. **26**(7), 2374–2381 (2014)
50. Ghidiu, M., et al.: Ion-exchange and cation solvation reactions in Ti3C2 MXene. Chem. Mater. **28**(10), 3507–3514 (2016)
51. Mashtalir, O., et al.: Intercalation and delamination of layered carbides and carbonitrides. Nat. Commun. **4**, 1716 (2013)
52. Mashtalir, O., et al.: Amine-assisted delamination of Nb2C MXene for Li-ion energy storage devices. Adv. Mater. **27**(23), 3501–3506 (2015)
53. Omomo, Y., et al.: Redoxable nanosheet crystallites of MnO2 derived via delamination of a layered manganese oxide. J. Am. Chem. Soc. **125**(12), 3568–3575 (2003)
54. Naguib, M., et al.: Large-scale delamination of multi-layers transition metal carbides and carbonitrides "MXenes". Dalton Trans. **44**(20), 9353–9358 (2015)
55. Meshkian, R., et al.: Theoretical stability and materials synthesis of a chemically ordered MAX phase, Mo2ScAlC2, and its two-dimensional derivate Mo2ScC2 MXene. Acta Mater. **125**, 476–480 (2017)
56. Enyashin, A.N., Ivanovskii, A.L.: Structural and electronic properties and stability of MX enes Ti2C and Ti3C2 functionalized by methoxy groups. J. Phys. Chem. C **117**(26), 13637–13643 (2013)
57. Persson, I., et al.: Tailoring structure, composition, and energy storage properties of MXenes from selective etching of in-plane, chemically ordered MAX phases. Small **14**(17), 1703676 (2018)
58. Intikhab, S., et al.: Stoichiometry and surface structure dependence of hydrogen evolution reaction activity and stability of MoxC MXenes. J. Catal. **371**, 325–332 (2019)

59. Shuck, C.E., et al.: Effect of Ti3AlC2 MAX phase on structure and properties of resultant Ti3C2Tx MXene. ACS Appl. Nano Mater. (2019)
60. Khazaei, M., et al.: Novel electronic and magnetic properties of two-dimensional transition metal carbides and nitrides. Adv. Func. Mater. **23**(17), 2185–2192 (2013)
61. Miranda, A., et al.: Electronic properties of freestanding Ti3C2Tx MXene monolayers. Appl. Phys. Lett. **108**(3), 033102 (2016)
62. Halim, J., et al.: Electronic and optical characterization of 2D Ti2C and Nb2C (MXene) thin films. J. Phys. Condens. Matter **31**(16), 165301 (2019)
63. Cui, J., et al.: Strain-tunable electronic structures and optical properties of semiconducting MXenes. Nanotechnology **30**(34), 345205 (2019)
64. Lai, S., et al.: Surface group modification and carrier transport properties of layered transition metal carbides (Ti2CTx, T:–OH,–F and–O). Nanoscale **7**(46), 19390–19396 (2015)
65. Liu, H., et al.: A novel nitrite biosensor based on the direct electrochemistry of hemoglobin immobilized on MXene-Ti3C2. Sens. Actuators B Chem. **218**, 60–66 (2015)
66. Dai, C., et al.: Two-dimensional tantalum carbide (MXenes) composite nanosheets for multiple imaging-guided photothermal tumor ablation. ACS Nano **11**(12), 12696–12712 (2017)
67. Chen, X., et al.: Ratiometric photoluminescence sensing based on Ti 3 C 2 MXene quantum dots as an intracellular pH sensor. Nanoscale **10**(3), 1111–1118 (2018)
68. Rasool, K., et al.: Antibacterial Activity of Ti3C2T x MXene. ACS Nano **10**(3), 3674–3684 (2016)
69. Huang, K., et al.: Two-dimensional transition metal carbides and nitrides (MXenes) for biomedical applications. Chem. Soc. Rev. **47**(14), 5109–5124 (2018)
70. Xue, Q., et al.: Photoluminescent Ti3C2 MXene quantum dots for multicolor cellular imaging. Adv. Mater. **29**(15), 1604847 (2017)
71. Zhou, L., et al.: Titanium carbide (Ti3C2Tx) MXene: a novel precursor to amphiphilic carbide-derived graphene quantum dots for fluorescent ink, light-emitting composite and bioimaging. Carbon **118**, 50–57 (2017)
72. Cai, Y., et al.: Diketopyrrolopyrrole–triphenylamine organic nanoparticles as multifunctional reagents for photoacoustic imaging-guided photodynamic/photothermal synergistic tumor therapy. ACS Nano **11**(1), 1054–1063 (2017)
73. Naunheim, K.S., et al.: Preoperative chemotherapy and radiotherapy for esophageal carcinoma. J. Thorac. Cardiovasc. Surg. **103**(5), 887–895 (1992)
74. Robinson, J.T., et al.: Ultrasmall reduced graphene oxide with high near-infrared absorbance for photothermal therapy. J. Am. Chem. Soc. **133**(17), 6825–6831 (2011)
75. Bashkatov, A., et al.: Optical properties of human skin, subcutaneous and mucous tissues in the wavelength range from 400 to 2000 nm. J. Phys. D Appl. Phys. **38**(15), 2543 (2005)
76. Li, X., et al.: Carbon and graphene quantum dots for optoelectronic and energy devices: a review. Adv. Func. Mater. **25**(31), 4929–4947 (2015)
77. Ross, R.B., et al.: Endohedral fullerenes for organic photovoltaic devices. Nat. Mater. **8**(3), 208 (2009)
78. Arico, A.S., et al.: Nanostructured materials for advanced energy conversion and storage devices. In: Materials For Sustainable Energy: A Collection of Peer-Reviewed Research and Review Articles from Nature Publishing Group, pp. 148–159. World Scientific (2011)
79. Rakhi, R.B., et al.: Effect of postetch annealing gas composition on the structural and electrochemical properties of Ti2CT x MXene electrodes for supercapacitor applications. Chem. Mater. **27**(15), 5314–5323 (2015)
80. Xie, Y., et al.: Prediction and characterization of MXene nanosheet anodes for non-lithium-ion batteries. ACS Nano **8**(9), 9606–9615 (2014)
81. Yu, X., et al.: Ti3C2 MXene nanoparticles modified metal oxide composites for enhanced photoelectrochemical water splitting. Int. J. Hydrog. Energy **44**(5), 2704–2710 (2019)
82. Chen, X., et al.: Ti3C2 MXene quantum dots/TiO2 inverse opal heterojunction electrode platform for superior photoelectrochemical biosensing. Sens. Actuators B Chem. (2019)

83. Yan, D., et al.: A BiVO4 film photoanode with re-annealing treatment and 2D thin Ti3C2TX flakes decoration for enhanced photoelectrochemical water oxidation. Chem. Eng. J. **361**, 853–861 (2019)
84. Peng, X., et al.: Two dimensional nanomaterials for flexible supercapacitors. Chem. Soc. Rev. **43**(10), 3303–3323 (2014)
85. Portet, C., et al.: High power density electrodes for carbon supercapacitor applications. Electrochim. Acta **50**(20), 4174–4181 (2005)
86. Zhang, L.L., Zhou, R., Zhao, X.: Graphene-based materials as supercapacitor electrodes. J. Mater. Chem. **20**(29), 5983–5992 (2010)
87. Kaempgen, M., et al.: Printable thin film supercapacitors using single-walled carbon nanotubes. Nano Lett. **9**(5), 1872–1876 (2009)
88. Syamsai, R., Grace, A.N.: Ta4C3 MXene as supercapacitor electrodes. J. Alloy. Compd. **792**, 1230–1238 (2019)
89. Wu, W., et al.: Enhanced electrochemical performances of organ-like Ti3C2 MXenes/polypyrrole composites as supercapacitors electrode materials. Ceram. Int. **45**(6), 7328–7337 (2019)
90. Tang, Q., Zhou, Z., Shen, P.: Are MXenes promising anode materials for Li ion batteries? Computational studies on electronic properties and Li storage capability of Ti3C2 and Ti3C2X2 (X = F, OH) monolayer. J. Am. Chem. Soc. **134**(40), 16909–16916 (2012)
91. Sun, D., et al.: Two-dimensional Ti3C2 as anode material for Li-ion batteries. Electrochem. Commun. **47**, 80–83 (2014)
92. Wang, Y., et al.: Fe 3 O 4@ Ti 3 C 2 MXene hybrids with ultrahigh volumetric capacity as an anode material for lithium-ion batteries. J. Mater. Chem. A **6**(24), 11189–11197 (2018)
93. Seh, Z.W., et al.: Two-dimensional molybdenum carbide (MXene) as an efficient electrocatalyst for hydrogen evolution. ACS Energy Lett. **1**(3), 589–594 (2016)
94. Wang, Y., et al.: Graphene/carbon black hybrid film for flexible and high rate performance supercapacitor. J. Power Sources **271**, 269–277 (2014)
95. Yang, C., et al.: All-solid-state asymmetric supercapacitor based on reduced graphene oxide/carbon nanotube and carbon fiber paper/polypyrrole electrodes. J. Mater. Chem. A **2**(5), 1458–1464 (2014)
96. Gao, H., et al.: Flexible all-solid-state asymmetric supercapacitors based on free-standing carbon nanotube/graphene and Mn3O4 nanoparticle/graphene paper electrodes. ACS Appl. Mater. Interfaces. **4**(12), 7020–7026 (2012)
97. Xu, Y., et al.: Flexible solid-state supercapacitors based on three-dimensional graphene hydrogel films. ACS Nano **7**(5), 4042–4049 (2013)
98. Wu, Q., et al.: Supercapacitors based on flexible graphene/polyaniline nanofiber composite films. ACS Nano **4**(4), 1963–1970 (2010)
99. Levitt, A.S., et al.: Electrospun MXene/carbon nanofibers as supercapacitor electrodes. J. Mater. Chem. A **7**(1), 269–277 (2019)
100. Zhan, C., et al.: Computational discovery and design of MXenes for energy applications: status, successes, and opportunities. ACS Appl. Mater. Interfaces (2019)
101. Velpula, G., et al.: Graphene meets ionic liquids: fermi level engineering via electrostatic forces. ACS Nano (2019)
102. Wang, X., et al.: Two-dimensional V4C3 MXene as high performance electrode materials for supercapacitors. Electrochim. Acta **307**, 414–421 (2019)